Chapter 17

Comparative Review Study on Elastic Properties Modeling for Unidirectional Composite Materials

Rafic Younes, Ali Hallal, Farouk Fardoun and Fadi Hajj Chehade

Additional information is available at the end of the chapter

http://dx.doi.org/10.5772/50362

1. Introduction

Due to the outstanding properties of 2D and 3D textile composites, the use of 3D fiber reinforced in high-tech industrial domains (spatial, aeronautic, automotive, naval, etc…) has been expanded in recent years. Thus, the evaluation of their elastic properties is crucial for the use of such types of composites in advanced industries. The analytical or numerical modeling of textile composites in order to evaluate their elastic properties depend on the prediction of the elastic properties of unidirectional composite materials with long fibers composites "UD". UD composites represent the basic element in modeling all laminates or 2D or 3D fabrics. They are considered as transversely isotropic materials composed of two phases: the reinforcement phase and the matrix phase. Isotropic fibers (e.g. glass fibers) or anisotropic fibers (e.g. carbon fibers) represent the reinforcement phase while, in general, isotropic materials (e.g. epoxy, ceramics, etc…) represent the matrix phase (Figure 1).

The effective stiffness and compliance matrices of a transversely isotropic material are defined in the elastic regime by five independent engineering constants: longitudinal and transversal Young's moduli E_{11} and E_{22}, longitudinal and transversal shear moduli G_{12} and G_{23}, and major Poisson's ratio ν_{12} (Noting that direction 1 is along the fiber). The minor Poisson's ratio ν_{23} is related to E_{22} and G_{12}. The effective elastic properties are evaluated in terms of mechanical properties of fibers and matrix (Young's and shear moduli, Poisson's ratios and the fiber volume fraction V^f). The compliance matrix [S] of a transversely isotropic material is given as follow:

$$[S] = \begin{bmatrix} 1/E_{11} & -\nu_{12}/E_{11} & -\nu_{12}/E_{11} & 0 & 0 & 0 \\ -\nu_{12}/E_{11} & 1/E_{22} & -\nu_{23}/E_{22} & 0 & 0 & 0 \\ -\nu_{12}/E_{11} & -\nu_{23}/E_{22} & 1/E_{22} & 0 & 0 & 0 \\ 0 & 0 & 0 & 1/G_{23} & 0 & 0 \\ 0 & 0 & 0 & 0 & 1/G_{12} & 0 \\ 0 & 0 & 0 & 0 & 0 & 1/G_{12} \end{bmatrix}$$

The stiffness matrix [C] is the invers of the compliance matrix [S].

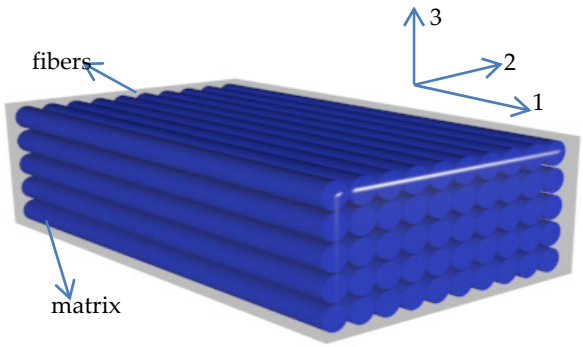

Figure 1. Unidirectional Composite.

In this chapter, a review of most known available analytical micromechanical models is presented in the second section of this chapter. Investigated models belonged to different categories: phenomenological models, semi-empirical models, elasticity approach models and homogenization models. In addition, the evaluation of elastic properties of UD composites using numerical FE method is investigated. Boundary, symmetric and periodic conditions, with different unit cells (square, hexagonal and diamond arrays), are discussed. In the third section, a comparison of the results obtained by the investigated analytical and numerical models is compared to available experimental data for different kinds of UD composites.

2. Review

The prediction of the mechanical properties of UD composites has been the main objective of many researches. Various micromechanical models have been proposed to evaluate the elastic properties of UD composites. These models could be divided into four categories: phenomenological models, elasticity approach models, semi-empirical models and homogenization models.

2.1. Phenomenological models

2.1.1. Rule of Mixture "ROM"

The well-known models that have been proposed and used to evaluate the properties of UD composites are the Voigt [1] and Reuss [2] models. The Voigt model is also known as the rule of mixture model or the iso-strain model, while the Reuss model is also known as the invers rule of mixture model or the iso-stress model.

Elastic properties are extracted from the two models where they are given under the rule of mixture (ROM) and the invers rule of mixture models (IROM).

$$E_{11} = V^f . E_{11}^f + V^m . E^m \quad \text{(from Voigt model)}$$

$$\nu_{12} = V_f \, \upsilon_{11}^f + V_m \, \upsilon^m \text{ (from Voigt model)}$$

$$E_{22} = \frac{E_{22}^f . E^m}{E^m . V^f + E_{22}^f . V^m} \quad \text{(from Reuss model)}$$

$$G_{12} = \frac{G_{12}^f . G^m}{G^m . V^f + G_{12}^f . V^m} \quad \text{(from Reuss model)}$$

2.2. Semi-empirical models

Semi empirical models have emerged to correct the ROM model where correcting factors are introduced. Under this category, it's noticed three important models: the modified rule of mixture, the Halpin-Tsai model [3] and Chamis model [4].

2.2.1. Modified Rule of Mixture (MROM)

While the investigations show that the obtained results by the ROM model for E_{11} and ν_{12} are in good agreement with experimental and finite element data, the results for E_{22} and G_{12} do not agree well with experimental and finite element data. Corrections have been made for E_{22} and G_{12}.

$$\frac{1}{E_{22}} = \frac{\eta^f . V^f}{E_{22}^f} + \frac{\eta^m . V^m}{E^m}$$

Where factors η^f, η^m are calculated as:

$$\eta^f = \frac{E_{11}^f . V^f + \left[\left(1 - \nu_{12}^f . \nu_{21}^f\right) . E^m + \nu^m . \nu_{21}^f . E_{11}^f\right] . V^m}{E_{11}^f . V^f + E^m . V^m}$$

$$\eta^m = \frac{\left[\left(1 - \nu^{m^2}\right) . E_{11}^f - \left(1 - \nu^m . \nu_{12}^f\right) . E^m\right] . V^f + E^m . V^m}{E_{11}^f . V^f + E^m . V^m}$$

$$\frac{1}{G_{12}} = \frac{\frac{V^f}{G_{12}^f} + \frac{\eta' . V^m}{G^m}}{V^f + \eta' . V^m}$$

With $0 < \eta' < 1$, (it is preferred to take $\eta' = 0.6$)

2.2.2. Halpin–Tsai model [3]

The Halpin-Tsai model also emerged as a semi-empirical model that tends to correct the transversal Young's modulus and longitudinal shear modulus. While for E_{11} and ν_{12}, the rule of mixture is used.

$$E_{22} = E^m.\left(\frac{1+\zeta\eta V_f}{1-\eta V_f}\right); G_{12} = G^m.\left(\frac{1+\zeta\eta V_f}{1-\eta V_f}\right)$$

$$\text{with } \eta = \left(\frac{M_f/M_m - 1}{M_f/M_m + \zeta}\right)$$

with $\zeta = 1$ and 2, and M = E or G for E_{22} and G_{12} respectively.

2.2.3. Chamis model [4]

The Chamis micromechanical model is the most used and trusted model which give a formulation for all five independent elastic properties. It's noticed in this model that E_{11} and ν_{12} are also predicted in the same maner of the ROM model, while for other moduli, V^f is replaced by its square root.

$$E_{11} = V^f\ E_{11}^f + V^m\ E^m$$

$$E_{22} = \frac{E^m}{1-\sqrt{V^f}\left(1-E^m/E_{22}^f\right)}$$

$$\nu_{12} = V^f\ \nu_{12}^f + V^m\ \nu^m$$

$$G_{12} = \frac{G^m}{1-\sqrt{V^f}\left(1-G^m/G_{12}^f\right)}$$

$$G_{23} = \frac{G^m}{1-\sqrt{V^f}\left(1-G^m/G_{23}^f\right)}$$

2.3. Elasticity approach models

Under this category, Hashin and Rosen [5] initially proposed a composite cylinder assemblage model (CCA) to evaluate the elastic properties of UD composites. Moreover, Christensen proposed a generalized self-consistent model [6] in order to better evaluate the transversal shear modulus G_{23}.

$$E_{11} = V^f\ E_{11}^f + V^m\ E^m + \frac{4.V^f.V^m.(\nu_{12}^f-\nu^m)^2}{\frac{V^f}{K^m}+\frac{1}{G^m}+\frac{V^m}{K^f}} \text{ (Hashin and Rosen [5])}$$

$$\nu_{12} = V^f\ .\nu_{12}^f + V^m\nu^m + \frac{V^fV^m\left(\nu_{12}^f-\nu^m\right)\left(\frac{1}{K^m}-\frac{1}{K^f}\right)}{\frac{V^f}{K^m}+\frac{1}{G^m}+\frac{V^m}{K^f}} \text{ (Hashin and Rosen [5])}$$

$$G_{12} = G^m.\frac{G^f.(1+V^f)+G^m.V^m}{G^f.V^m+G_m(1+V^f)} \text{ (Hashin and Rosen [5])}$$

G_{23} is the solution of the following equation: (Christensen [6])

$$A\left(\frac{G_{23}}{G_m}\right)^2 + 2B\left(\frac{G_{23}}{G_m}\right) + C = 0$$

With:

$$A = 3V^f.\left(1-V^f\right)^2.\left(\frac{G_{23}^f}{V^m}-1\right)\left(\frac{G_{23}^f}{G^m}+\eta_f\right)$$

$$+\left[\frac{G_{23}^f}{G^m}\eta_m+\eta_f\eta_m-\left(\frac{G_{23}^f}{G^m}\eta_m-\eta_f\right)V^{f^3}\right].\left[V_f\eta_m\left(\frac{G_{23}^f}{G^m}-1\right)-\left(\frac{G_{23}^f}{G^m}\eta_m+1\right)\right]$$

$$B = -3V^f V^{m^2}\left(\frac{G_{23}^f}{G^m}-1\right)\left(\frac{G_{23}^f}{G^m}+\eta_f\right)+\frac{V^f}{2}(\eta_m+1)\left(\frac{G_{23}^f}{G^m}-1\right)\left[\frac{G_{23}^f}{G^m}+\eta_f+\left(\frac{G_{23}^f}{G^m}\eta_m-\eta_f\right)V^{f^3}\right]$$

$$+\left\{\frac{1}{2}\left[\frac{G_{23}^f}{G^m}\eta_m-\left(\frac{G_{23}^f}{G^m}-1\right)V^f+1\right].\left[(\eta_f-1)\left(\frac{G_{23}^f}{G^m}+\eta_f\right)-2\left(\frac{G_{23}^f}{G^m}\eta_m-\eta_f\right)V^{f^3}\right]\right\}$$

$$C = -3V^f V^{m^2}\left(\frac{G_{23}^f}{G^m}-1\right)\left(\frac{G_{23}^f}{G^m}+\eta_f\right)+\left[\frac{G_{23}^f}{G^m}\eta_m+\left(\frac{G_{23}^f}{G^m}-1\right)V^f+1\right]\left[\frac{G_{23}^f}{G^m}+\eta_f+\left(\frac{G_{23}^f}{G^m}\eta_m-\eta_f\right)V^{f^3}\right]$$

With

$$\eta_m = 3-\nu_m\,;\eta_f = 3-\nu_{23}^f$$

$K_f = \frac{E_f}{2(1-2\nu_f)(1+\nu_f)}$ and $K_m = \frac{E_m}{2(1-2\nu_m)(1+\nu_m)}$ are the bulk modulus of the fiber and the matrix under longitudinal strain respectively .

$$\nu_{23} = \frac{K-m.G_{23}}{K+m.G_{23}};\ \text{with m} = 1+4\text{K}.\frac{\nu_{12}^2}{E_{11}}$$

K is the bulk modulus of the composite under longitudinal strain

$$\text{K} = \frac{K^m.(K^f+G^m).V^m+K^f.(K^m+G^m).V^f}{(K^f+G^m).V^m+(K^m+G^m).V^f}$$

$$E_{22} = 2.(1+\nu_{23}).G_{23}$$

2.4. Homogenization models

2.4.1. Mori-Tanaka model (M-T)

The Mori-Tanaka model is initially developed by Mori and Tanaka [7]. This is a well-known model which is widely used for modeling different kinds of composite materials. This is an inclusion model, where fibers are simulated by inclusions embedded in a homogeneous medium. The Benveniste formulation [8] for the Mori-Tanaka model is given by:

$$\text{C}_{\text{MT}} = \text{C}_\text{m} + \left[\text{V}_\text{f}.\langle(\text{C}_\text{f}-\text{C}_\text{m}).\text{A}_{\text{Eshelby}}\rangle\right].\left[\text{V}_\text{m}.\text{I}+\text{V}_\text{f}.\langle\text{A}_{\text{Eshelby}}\rangle\right]^{-1}$$

With C_m and C_f are the stiffness matrices of the matrix phase and the reinforcement phase (inclusions) respectively. V_f and V_m are the volume fractions of the matrix phase and the reinforcement phase (inclusions) respectively. $\text{A}_{\text{Eshelby}}$ is the strain concentration tensor of the dilute solution presented by:

$$A_{Eshelby} = [I + E.C_m^{-1}.(C_f - C_m)]^{-1}$$

With E is the Eshelby tensor which depends on the shape of the inclusion and the Poisson's ratio of the matrix. More detailed information about the Eshelby tensor could be found in Mura [9]. The Eshelby tensor is then calculated for each inclusion along with the stiffness matrix.

2.4.2. Self-consistent model (S-C)

The self-consistent model has been proposed by Hill [10] and Budianski [11] to predict the elastic properties of composite materials reinforced by isotropic spherical particulates. Later the model was presented and used to predict the elastic properties of short fibers composites [12]. In this study the potential of the S-C model will be investigated when applied on UD composites with long fibers. The S-C model is an iterative model yielding the stiffness matrix as follows:

At the first iteration, fibers which represent the inclusions are supposed surrounded by an isotropic matrix, thus the S-C model is similar to the Eshelby dilute solution model. Then, at the second iteration, the inclusions are considered to be embedded in homogeneous medium which supposed to have the stiffness matrix similar to that of the composite calculated at the first iteration.

First iteration:

$$A_{Eshelby} = [I + E.C_m^{-1}.(C_f - C_m)]^{-1}$$

$$C_{sc} = C_m + \left[V_f.\langle (C_f - C_m).A_{Eshelby}\rangle\right]$$

Second iteration:

$$A_{Eshelby} = [I + E.C_{sc}^{-1}.(C_f - C_{sc})]^{-1}$$

$$C_{sc} = C_m + \left[V_f.\langle (C_f - C_m).A_{Eshelby}\rangle\right]$$

2.4.3. Bridging model

Recently, a new micromechanical model has been proposed by Huang et al. [13,14]. The model is developed to predict the stiffness and the strength of UD composites. The elastic properties by the bridging model is given as follows:

$$E_{11} = V_f.E_{11}^f + V_m.E_m$$

$$E_{22} = \frac{(V_f+V_m.a_{11})(V_f+V_m.a_{22})}{(V_f+V_m.a_{11})(V_f.S_{11}^f+V_m.a_{22}.S_{22}^m)+V_f.V_m(S_{21}^m-S_{21}^f)a_{12}}$$

$$V_{12} = V_f\,v_{11}^f + V_m\,v_m$$

$$G_{12} = \frac{(V_f+V_m.a_{66})G_{12}^f G_m}{V_f.G_m+V_m.a_{66}.G_{12}^f}$$

$$G_{23} = \frac{0.5(V_f + V_m.a_{44})}{V_f(S_{22}^f - S_{23}^f) + V_m.a_{44}(s_{22}^m - s_{23}^m)}$$

With a_{ij} are the components of the bridging matrix A, [13,14].

S_{ij}^f and and S_{ij}^m are the components of the compliance matrices of the fibers and the matrix respectively.

2.5. Numerical FE modeling

The numerical FE modeling is widely used in predicting the mechanical properties of composites. The numerical modeling is a reliable tool, but the time consumed on the geometrical dimensions definition and the corresponding calculation time, represent a major disadvantage against analytical models. Moreover there are many discussions and studies that deal with the appropriate boundary, symmetric and periodic conditions required to evaluate the elastic properties of UD composites. In this domain, a major work is done by S. Li [15]. It should be noticed that the numerical FE modeling require geometrical modeling or representation of the REV. while for UD composites, there are three types of fiber arrangements: square array, diamond array and hexagonal array (Figure 2).

In order to investigate the numerical FE modeling, the modeling of a quarter unit cell for a square array, diamond array and hexagonal array is conducted using Comsol Multiphysics software. A tetrahedral meshing is used. The resumed boundary conditions applied are given in (Table 1). Note that U, V and W are the displacements along 1, 2 and 3 directions respectively applied on the X+, X-, Y+, Y-, Z+ and Z- faces (with X faces are orthogonal to the fiber direction 1).

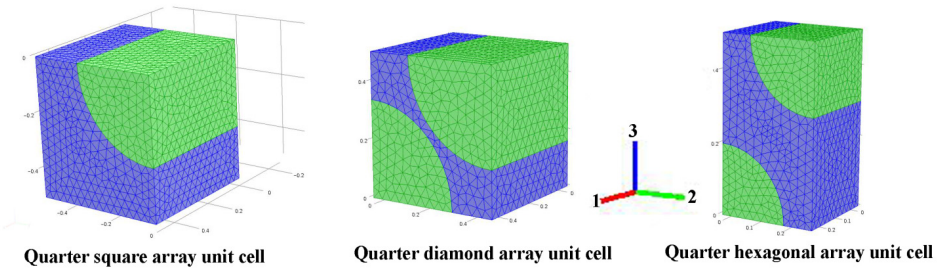

Figure 2. Meshing of square, diamond and hexagonal array unit cells.

After applying boundary conditions and the displacement constant K, the corresponding engineering constants are calculated as follow, in terms of corresponding stresses and strains (σ_{11}, σ_{22}, τ_{12}, τ_{23}, ε_{11}, ε_{22}, Υ_{12} and Υ_{23}):

On the X+ face:

$E_{11} = \frac{\sigma_{11}}{\varepsilon_{11}}$, where $\sigma_{11}$and ε_{11} are calculated numerically on the X+ face

On the Y+ face:

$E_{22} = \frac{\sigma_{22}}{\varepsilon_{22}}$, where σ_{22} and ε_{22} are calculated numerically on the Y+ face

On the X+ face:

$G_{12} = \frac{\tau_{12}}{\Upsilon_{12}}$, where τ_{12} and Υ_{12} are calculated numerically on the X+ face

On the Z+ face:

$G_{23} = \frac{\tau_{23}}{\Upsilon_{23}}$, where $\tau_{23}$and Υ_{23} are calculated numerically on the Z+ face

	X faces		Y faces		Z faces	
	X-	X+	Y-	Y+	Z-	Z+
E_{11} and ν_{12}	U = 0, V and W free	U = K, V and W free	V = 0, U and W free	U, V and W free	W = 0, U and V free	U, V and W free
E_{22} and ν_{23}	U = 0, V and W free	U, V and W free	V = 0, U and W free	V = K, U and W free	W = 0, U and V free	U, V and W free
G_{12}	V = W = 0	V = K W= 0	U = W = 0	U=W = 0	W = 0	W = 0
G_{23}	U = 0	U = 0	U = W = 0	U = W = 0	U = V = 0	U = 0 V= K

Table 1. Boundary conditions on the X, Y and Z faces of the quarter unit cell.

3. Comparative study, analysis and discussion

3.1. Results

In this section, a comparison of analytical models and numerical models with available experimental data is presented. Three different kinds of UD composites are taken as examples: Glass/epoxy composite [16], carbon/epoxy composite [14] and polyethylene/epoxy composite [17] (Table 2). The glass fibers are isotropic fibers while the carbon and the polyethylene fibers are transversely isotropic fibers. Knowing that the epoxy matrices are assumed isotropic, it's well noticed that for the polyethylene/epoxy, the Young's modulus of the epoxy is higher than that transversal modulus of the fibers, which represent an important case to be investigated.

Fibers	E_{11}^f (GPa)	E_{22}^f (GPa)	G_{12}^f (GPa)	ν_{12}^f	ν_{23}^f
E-Glass [16]	73.1	73.1	29.95	0.22	0.22
Carbon [14]	232	15	24	0.279	0.49
Polyethylene [17]	60.4	4.68	1.65	0.38	0.55
Matrix	E^m (GPa)		G^m (GPa)	ν^m	
Epoxy resin [16]	3.45	3.45	1.28	0.35	0.35
Epoxy [14]	5.35	5.35	1.97	0.354	0.354
Epoxy [17]	5.5	5.5	1.28	0.37	0.37

Table 2. Elastic properties of the fibers and epoxy matrices.

3.1.1. Longitudinal Young's modulus E_{11}

For the longitudinal Young's modulus E_{11}, obtained analytical and numerical results are compared to those available experimental data for carbon/epoxy and polyethylene/epoxy UD composites in terms of the fiber volume fraction Vf. Investigated analytical models belong to the ROM, the Elasticity approach model (EAM), M-T and S-C models. Please note that ROM, MROM, Chamis, Halpin-Tsai and Bridging models share the same formulation for E_{11}.

It's well noticed that the predicted results for all investigated models are in good agreement with the experimental data for both composites with different V^f (Figure 3 and 4).

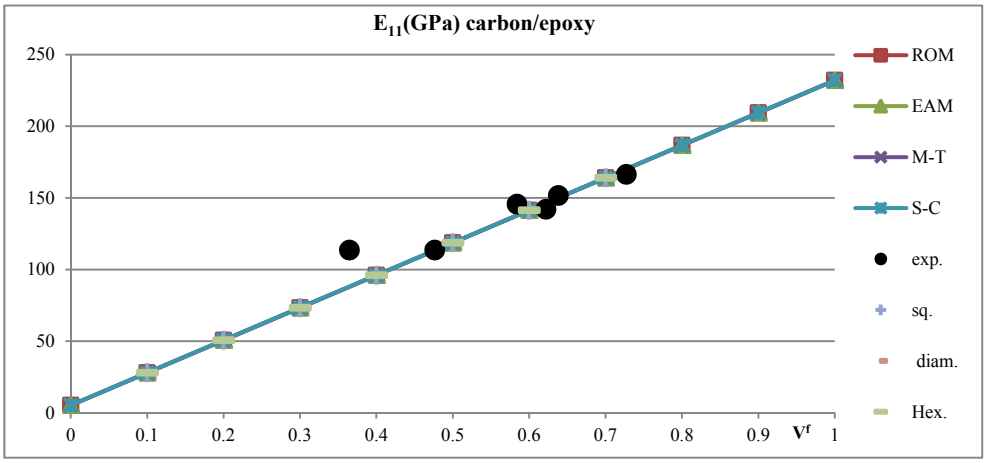

Figure 3. Predicted analytical, numerical and experimental results for E_{11} in terms of V^f.

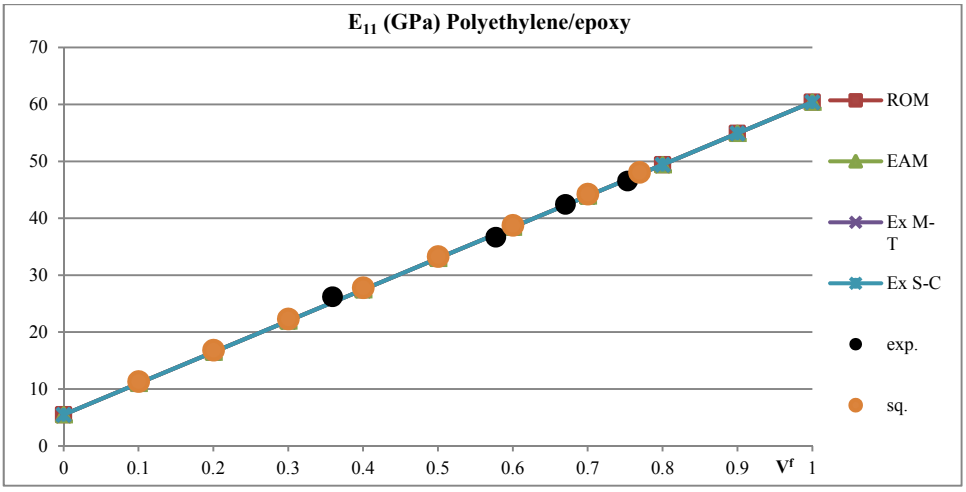

Figure 4. Predicted analytical, numerical and experimental results for E_{11} in terms of V^f.

3.1.2. Transversal Young's modulus E_{22}

The prediction of the transversal Young's modulus and in contrast with the longitudinal modulus presents a real challenge for the researchers. Thus, many analytical models are proposed belonged to different micromechanics approach. In addition, the potential of the FE element modeling is investigated. Predicted results of different analytical and numerical models for three UD composites are presented in figures (5,6 and 7)

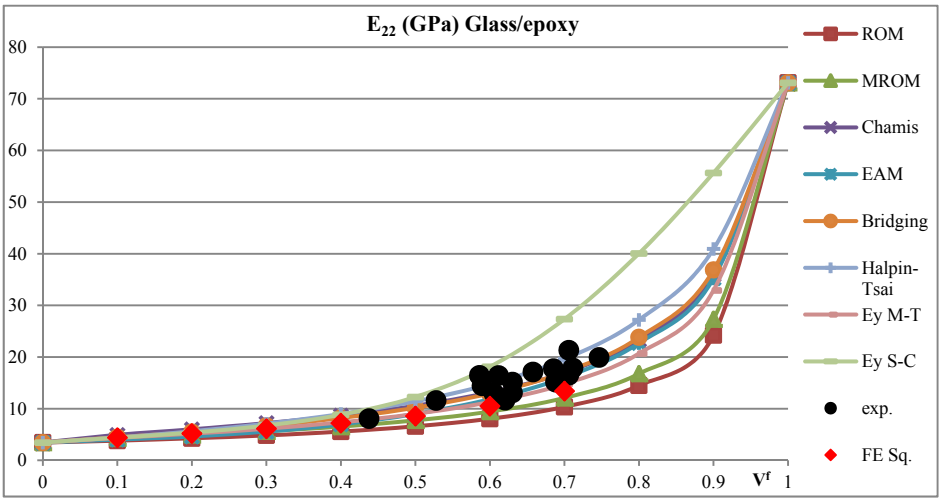

Figure 5. Predicted analytical, numerical and experimental results for E_{22} in terms of V^f.

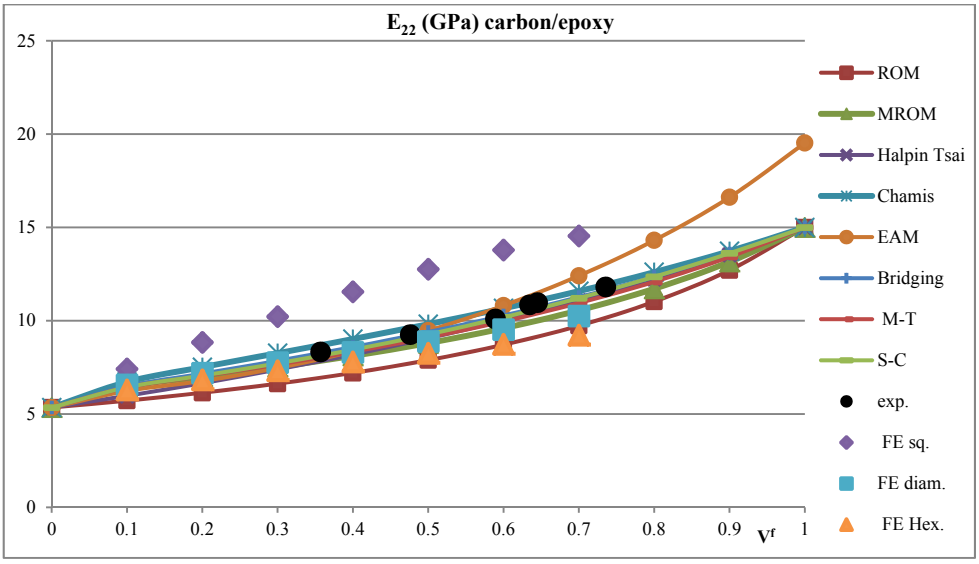

Figure 6. Predicted analytical, numerical and experimental results for E_{22} in terms of V^f.

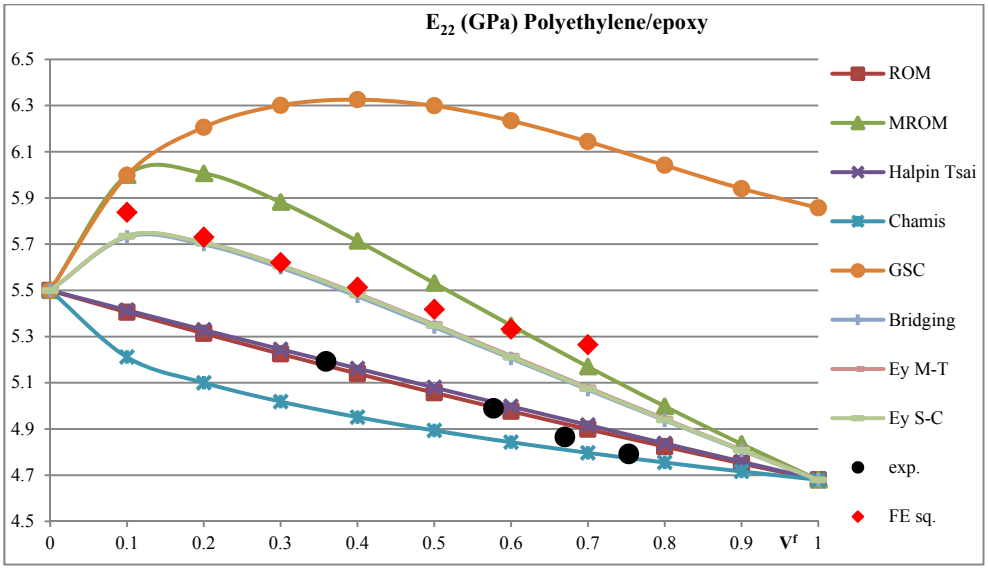

Figure 7. Predicted analytical, numerical and experimental results for E_{22} in terms of V^f.

It's shown that for the glass/epoxy composite, the S-C model overestimates the experimental results, while the ROM and MROM models underestimate it. Other analytical models, especially the Chamis, Bridging and EAM models yield results that correlate well with the available experimental data for different values of Vf. Moreover, it's noticed that the FE (Square array), the Halpin-Tsai and the M-T models gives good predictions. Concerning composites reinforced with transversely isotropic fibers, it's well remarked that the EAM model well overestimates E_{22} especially with the polyethylene/epoxy composite. The ROM underestimates the experimental results, while other analytical models, in addition to the numerical FE (diamond array) model, yield very good predictions for the carbon/epoxy composite. However, with the polyethylene/epoxy, it's noticed that only the results obtained from the ROM and the Halpin-Tsai models correlate well with the experimental data, while the Chamis model shows a good agreement with Vf higher than 0.6.

3.1.3. Longitudinal shear modulus G_{12}

Experimental results for two UD composites are used to be compared with. Figures 8 show clearly the MROM, EAM, Halpin-Tsai, Chamis, bridging analytical models, in addition to all numerical FE models yield very good results for the carbon/epoxy composite. However, it's remarked that the inclusion models, the M-T and S-C models, overestimate the longitudinal shear modulus. Concerning the polyethylene/epoxy composite, only results obtained results from the MROM and Chamis models agree well with the available experimental data (Figure 9).

3.1.4. *Transversal shear modulus G_{23}*

For the transversal shear modulus G_{23}, it's shown from Figure 10 and 11, that the bridging model yields the best results. In addition, it's remarked that the EAM, Chamis yield reasonable predictions underestimating the experimental data, while the M-T and S-C models overestimate it. Concerning the numerical modeling, predicted results always overestimate the available experimental results for the two composites.

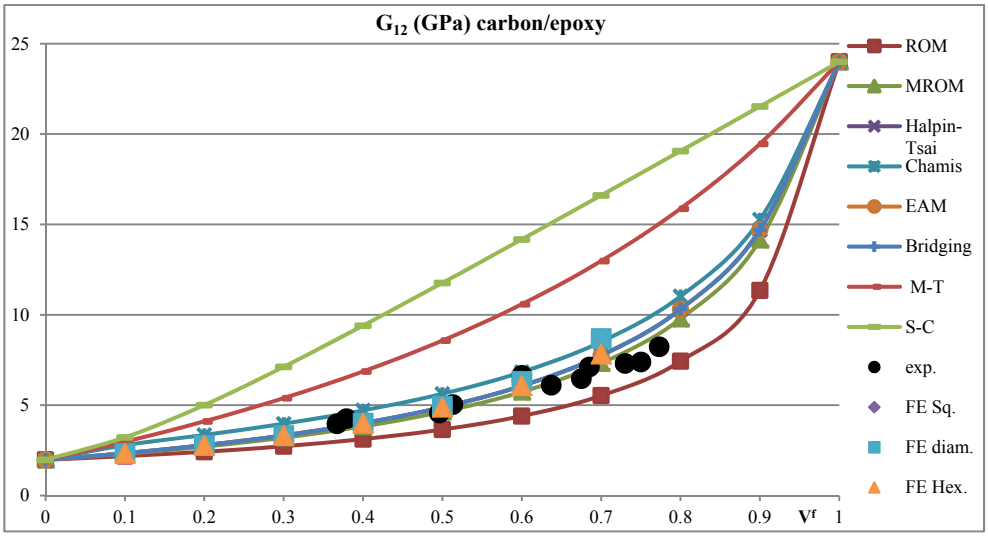

Figure 8. Predicted analytical, numerical and experimental results for G_{12} in terms of V^f.

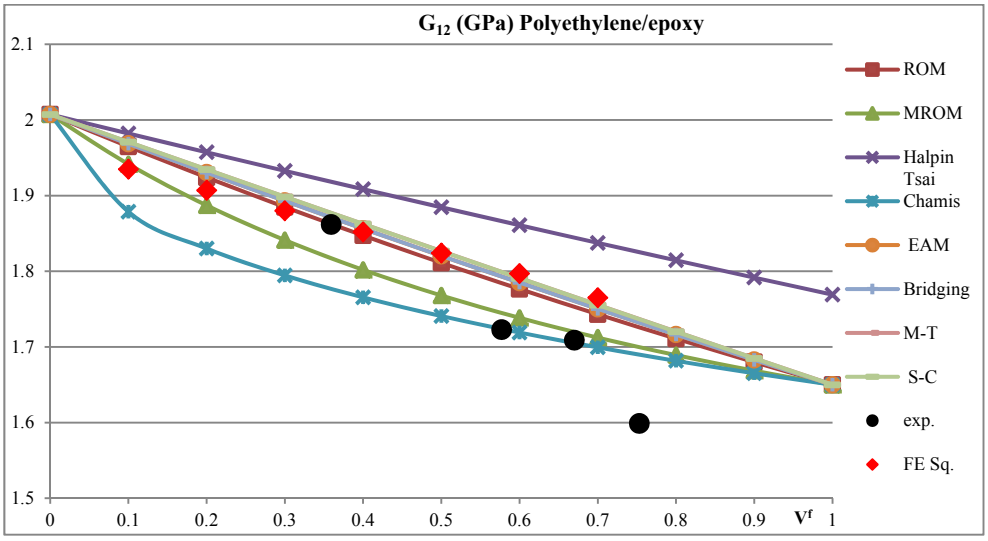

Figure 9. Predicted analytical, numerical and experimental results for G_{12} in terms of V^f.

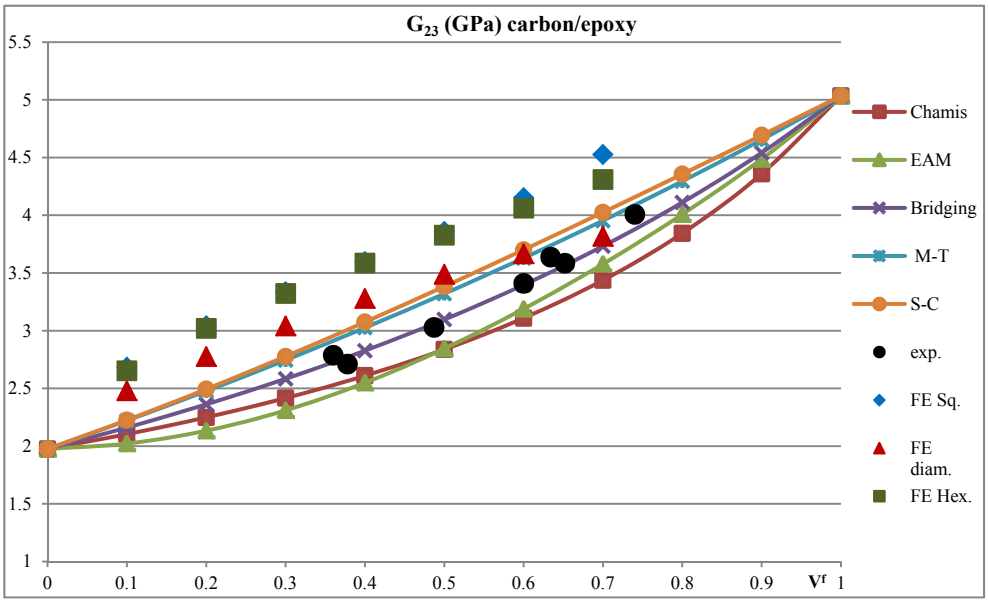

Figure 10. Predicted analytical, numerical and experimental results for G_{23} in terms of V^f.

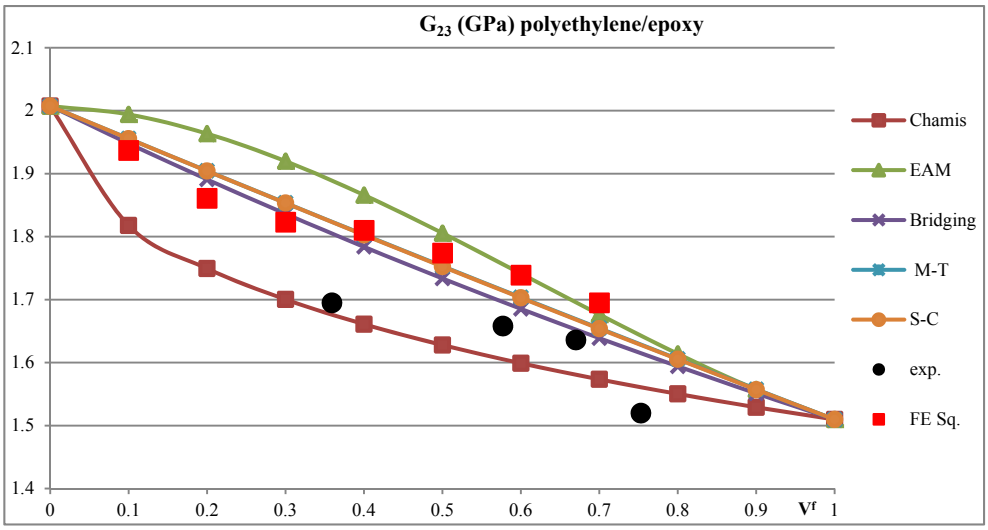

Figure 11. Predicted analytical, numerical and experimental results for G_{23} in terms of V^f.

3.1.5. Major Poisson's ratio ν_{12}

Concerning the Poisson's ratios, the obtained results of the analytical models are only compared to those numerical due the missing of experimental data for the studied UD composites. Figure 12 shows that for the major Poisson's ratio ν_{12}, all analytical and numerical models correlate well with each other.

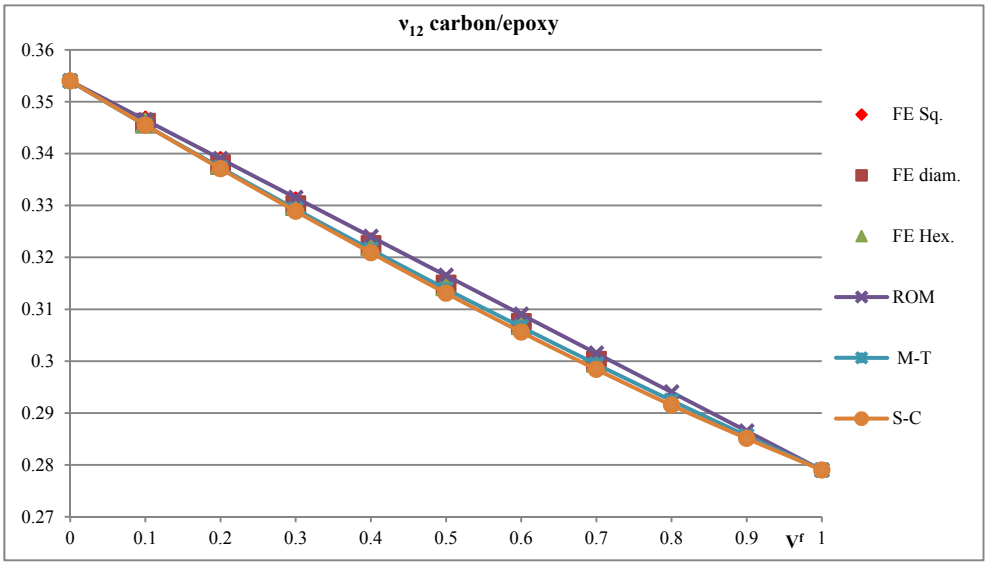

Figure 12. Predicted analytical and numerical results for ν_{12} in terms of V^f.

3.2. Analysis and discussion

In this section, an analysis of the predicted results for each model is presented apart. It's shown from the above results that for the phenomenological models, the Voigt and Reuss models, represented by the ROM model, show very good predictions for the longitudinal Young's modulus E_{11} and major Poisson's ratio ν_{12}. However, with for the transversal Young's modulus E_{22} the ROM model always underestimates the experimental results

except for the polyethylene/epoxy case where it's well agree with the available experimental data. Concerning the longitudinal shear modulus G_{12}, the ROM model didn't yield good prediction for both studied cases the carbon/epoxy and the polyethylene/epoxy composites.

As known the semi-empirical models have been emerged and proposed in order to correct the predictions of the ROM model for the transversal Young's and longitudinal shear moduli. While the investigated models share the same formulations for E_{11} and ν_{12} with ROM model, the corrections made for E_{22} and G_{12} prove to be effective. It's shown that the Chamis model yields very good results for all studied cases, while the MROM and Halpin-Tsai the models only suffer with the special case of the polyethylene/epoxy with the E_{22} and G_{12} respectively.

Concerning the elasticity approach models, the proposed formulation of the E_{11} yields similar results for that proposed by the ROM model. While for the transversal Young's modulus E_{22}, it's clearly noticed that with isotropic fibers, the model results correlate well with those experimental, while with the case of transversely isotropic fibers, reasonable predictions are shown for the carbon/epoxy case. However, for the polyethylene case the model well overestimates the experimental results. The reason could be conducted to that EAM models are initially proposed to deal with UD composites reinforced with isotropic fibers. For the longitudinal shear modulus G_{12}, the elastic solution formulation agrees well with the experimental data. Concerning the transversal shear modulus, the predictions made by the generalized self-consistent model of the Christensen model [6], which is developed to enhance the predictions of this elastic property, always overestimates the experimental data.

In this study, the potential of the homogenization models is investigated. The inclusion models, the M-T and the S-C models, and the bridging model, yield good prediction for both longitudinal Young's modulus and major Poisson's ratio. However, for the transversal Young's modulus E_{22}, reasonable agreement is shown for the glass/epoxy and carbon/epoxy cases, except with the self-consistent model which overestimates the experimental data for high V^f. While for the case of the polyethylene/epoxy, all three models yield almost the same results and overestimate the compared experimental data while agree with FE modeling results. The same problem is shown with the prediction of the shear moduli, where for the polyethylene/epoxy case, the models belonged to the homogenization approach give the same results overestimating the experimental data. While with the carbon/epoxy case, it's noticed that the bridging model predicts better the shear moduli, while the M-T and S-C models well overestimate the experimental data especially for the G_{12}.

Concerning the numerical modeling, it's well noticed that there are different predicted results for different arrays. It's also remarked, that the FE numerical modeling didn't yield better results than the analytical models, except for the longitudinal Young's modulus and major Poisson's ratio where all predicted results from numerical and analytical models correlate well with available experimental data.

4. Conclusion

In this study, the evaluated results, for the elastic properties, of most known analytical micromechanical models, as well as FE modeling methods, are compared to available experimental data for three different UD composites: Glass/epoxy, carbon/epoxy and polyethylene/epoxy. It should be noticed that the studied cases cover different kinds of reinforced composites by isotropic fibers (glass) and transversely isotropic fibers (carbon and polyethylene). In addition, the polyethylene/epoxy presents an interesting case study, where the matrix is stiffer than the fibers in the transvers direction.

The analyses of the compared results show clearly that all analytical and numerical models show a very good agreement for the longitudinal Young's modulus E_{11} and major Poisson's ratio ν_{12}. However, the other moduli, the transversal Young's modulus E_{22}, longitudinal shear modulus G_{12} and the transversal shear modulus G_{23}, represent the main challenge for the researchers. It's shown that analytical micromechanical models belonged to the semi-empirical models, especially the Chamis model, predict well these elastic properties. Moreover, the bridging model proves to be a reliable model when predicting the elastic properties of carbon/epoxy composite. It's noticed that almost all models suffer with the prediction of elastic properties for the polyethylene/epoxy composite. However, models belonged to the elasticity approach and inclusion approach (M-T and S-C models) show inconsistency in predicting the elastic properties of studied UD composites. Numerical models, based on the FE method, show that using different fibers arrangements will lead to different predicted results. Moreover, the FE didn't prove that it could be more accurate than some simple and straightforward analytical model. As a conclusion from this study, the Chamis model and the bridging model could be considered as the most complete models which could give quite accurate estimations for all five independent elastic properties. Noting that the corrections proposed by the Halpin-Tsai model, prove that it well enhance the prediction of the transversal Young's modulus E_{22}.

Author details

Rafic Younes*
LISV, University of Versailles Saint-Quentin, Versailles, France
Faculty of Engineering, Lebanese University, Rafic Hariri campus, Beirut, Lebanon

Ali Hallal
LISV, University of Versailles Saint-Quentin, Versailles, France
L3M2S, Lebanese University, Rafic Hariri campus, Beirut, Lebanon

Farouk Fardoun
L3M2S, Lebanese University, Rafic Hariri campus, Beirut, Lebanon

* Corresponding Author

Fadi Hajj Chehade
L3M2S, Lebanese University, Rafic Hariri campus, Beirut, Lebanon

5. References

[1] Voigt W. Uber die Beziehung zwischen den beiden Elastizitatskonstanten Isotroper Korper. Wied. Ann, 38 (1889) 573-587.
[2] Reuss A. Berechnung der Fliessgrense von Mischkristallen auf Grund der Plastizitätsbedingung für Einkristalle. Zeitschrift Angewandte Mathematik und Mechanik, 9 (1929) 49-58.
[3] Halpin JC, Kardos JL. The Halpin-Tsai equations: A review. Polymer Engineering and Science, May, 1976, Vol. 16, No. 5.
[4] Chamis CC. Mechanics of composite materials: past, present, and future. J Compos Technol Res ASTM 1989;11:3–14.
[5] Hashin Z, Rosen BW. The elastic moduli of fiber reinforced materials. Journal of Applied Mechanics, Trans ASME, 31 (1964). 223-232.
[6] Christensen RM. A critical evaluation for a class of micromechanics models. Journal of Mechanics and Physics of Solids 1990; 38(3):379–404.
[7] Mori T, Tanaka K. Average stress in matrix and average elastic energy of materials with misfitting inclusions, Acta Mettall. 21, 1973, 571-574.
[8] Benveniste Y. A new approach to the application of Mori-Tanaka's theory in composite materials. Mechanics of Materials, 6, 1987, 147-157.
[9] Mura T. Micromechanics of Defects in Solids, 2nd edn. Martinus Nijhof Publishers, Dordrecht, 1987.
[10] Hill R. Theory of mechanical properties of fibre-strengthen materials-III. Self-consistent model. Journal of Mechanics and Physics of Solids 1965; 13: 189-198.
[11] Budiansky B. On the elastic moduli of some heterogeneous materials, J. Mech. Phys. Solids 13, 1965, 223-227.
[12] Chou TW, Nomura S, Taya M. A self-consistent approach to the elastic stiffness of short-fiber composites, J. Compos Mater, 14, 1980, 178-188.
[13] Huang ZM. Simulation of the mechanical properties of fibrous composites by the bridging micromechanics model. Composites: Part A 32 (2001) 143–172.
[14] Huang ZM. Micromechanical prediction of ultimate strength of transversely isotropic fibrous composites. International Journal of Solids and Structures 38 (2001) 4147-4172.
[15] Li S. Boundary conditions for unit cells from periodic microstructures and their implications. Composites Science and Technology 68 (2008) 1962–1974.
[16] Shan HZ, Chou TW. Transverse elastic moduli of unidirectional fiber composites with fiber/matrix interfacial debonding. Composites Science and Technology 53 (1995) 383-391.

[17] Wilczynski AP, Lewinski J. Predecting the properties of unidirectional fibrous composites with monotropic reinforcement. Composite Science and Technology 55 (1995) 139-143